Received: 23 January 2023 | Revised: 3 August 2023 | Accepted: 20 August 2023

DOI: 10.1002/cbf.3843

RESEARCH ARTICLE

CELL BIOCHEMISTRY & FUNCTION WILEY

An in vitro investigation of L-kynurenine, quinolinic acid, and kynurenic acid on B16 F10 melanoma cell cytotoxicity and morphology

Charlise Basson[1] | June Cheptoo Serem[2] | Yvette Nkondo Hlophe[1] | Priyesh Bipath[1]

[1]Department of Physiology, School of Medicine, University of Pretoria, Pretoria, South Africa

[2]Department of Anatomy, School of Medicine, University of Pretoria, Pretoria, South Africa

Correspondence
Priyesh Bipath, Department of Physiology, School of Medicine, Faculty of Health Sciences, University of Pretoria, Private Bag X323, Gezina, Pretoria, Gauteng 0031, South Africa.
Email: priyesh.bipath@up.ac.za

Funding information
National Research Foundation; School of Medicine Research Committee; Research Development Program; University of Pretoria

Abstract

The metastatic behavior of melanoma has accentuated the need for specific therapy targets. Compounds, namely L-kynurenine (L-kyn), quinolinic acid (Quin), and kynurenic acid (KA) previously displayed antiproliferative and cytotoxic effects in vitro against cancer cells. Despite the growing interest in these compounds there are limited studies examining the in vitro effects on melanoma. In B16 F10 melanoma cells, RAW 264.7 macrophage cells, and HaCat keratinocyte cells, postexposure to the compounds, crystal violet staining was used to determine the half-maximal inhibitory concentration (IC_{50}), whereas polarization-optical transmitted light differential interference contrast and light microscopy after hematoxylin and eosin (H&E) staining was used to assess morphological changes. L-kyn, Quin, and KA-induced cytotoxicity in all cell lines, with L-kyn being the most cytotoxic compound. L-kyn and KA at IC_{50}-induced morphological changes in B16 F10, RAW 264.7, and HaCat cell lines, whereas Quin had effects on B16 F10 and RAW 264.7 cells but did not affect HaCat cells. L-kyn, Quin, and KA each display different levels of cytotoxicity, which were cell line specific. L-kyn was shown to be the most potent compound against all cell lines and may offer future treatment strategies when combined with other viable treatments against melanoma.

KEYWORDS
kynurenic acid, kynurenine metabolites, L-kynurenine, melanoma, quinolinic acid

1 | INTRODUCTION

Cancer is defined as a group of noncommunicable diseases[1] arising from a series of genetic mutations, which ultimately leads to alterations in the phenotypic, functional, and molecular characteristics of cells.[1,2] Genetic mutations involve tumor suppressor gene deactivation and/or the activation of proto-oncogenes,[3] which modifies cell cycle processes and contributes to uncontrolled proliferation in cancer cells.[4,5] The high proliferation rate of cancer cells can be attributed to their ability to reprogram their metabolism through a mechanism known as the Warburg effect.[6] Although the Warburg effect is characterized as an inefficient metabolic shift from mitochondrial oxidative phosphorylation (OXPHOS) to glycolysis,[7] it is necessary to support the biosynthetic requirements of uncontrolled proliferation and maintain a nicotinamide adenine dinucleotide (NAD^+)/nicotinamide adenine dinucleotide + hydrogen (NADH) redox ratio.[6,8] Cancer cells often present with higher NAD^+/

NADH and $NADP^+$/NADPH ratios compared to noncancerous cells, suggesting the important role of NAD^+ in cancer.[6] Nicotinamide adenine dinucleotide (NAD^+) is a cofactor in cellular reactions including ATP synthesis and DNA repair and is implicated in redox reactions for obtaining energy.[6,9]

Precursors of the NAD^+ production pathway can be obtained through dietary sources in the form of vitamin B_3/niacin (including nicotinic acid and nicotinamide).[10] Niacin's role in the skin has been well documented, as a deficiency can lead to pellagra (characterized by dermatitis) and an increased risk for UV-induced skin tumors. Increasing evidence suggest niacin's role in cancer, including processes involved in genomic instability, DNA repair, regulation of cell division, and apoptosis.[11] However, when NAD^+ levels are depleted due to insufficient dietary niacin intake or a compromised immune system, tryptophan is catabolized for NAD^+ de novo synthesis.[12,13]

Tryptophan is an essential amino acid in mammals[14] and the least abundant of all essential amino acids.[14] Tryptophan catabolism produces various metabolites, which act as active substances (Figure 1).[14] The

Significance statement

The kynurenine pathway is known to be activated in cancer. Metabolites in the kynurenine pathway, namely L-kynurenine (L-kyn), quinolinic acid (Quin), and kynurenic acid (KA) previously displayed antiproliferative and cytotoxic effects in vitro against cancer cells. Despite the growing interest in these compounds there are limited studies examining the in vitro effects on melanoma. This study provides a better understanding of the in vitro cytotoxic effects of kynurenine exogenous compounds against B16 F10 melanoma cells and confirms that L-kyn, Quin, and KA each display different levels of cytotoxicity. In addition, this study demonstrates that L-kyn is the most potent cytotoxic compound and may offer future treatment strategies in combination with other viable treatments against melanoma.

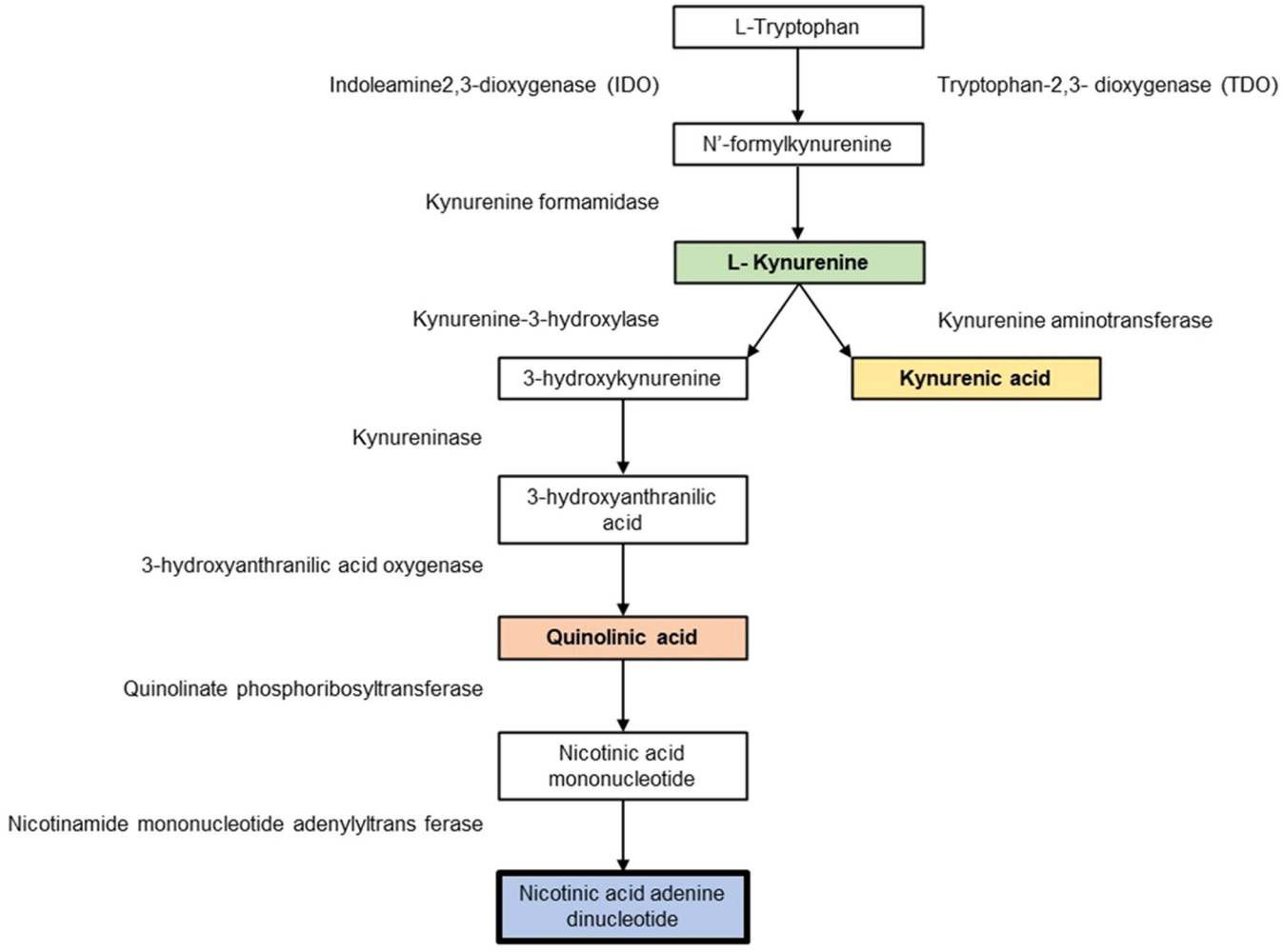

FIGURE 1 Tryptophan metabolism and the formation of kynurenine metabolites, leading to nicotinamide adenine dinucleotide (NAD^+) synthesis. L-tryptophan is cleaved by indoleamine 2,3 dioxygenase 1 (IDO1), indoleamine 2,3 dioxygenase 2 (IDO2) or tryptophan-2,3-dioxygenase (TDO) to yield *N′*-formylkynurenine, which is hydrolyzed by kynurenine formamidase to L-kynurenine (L-kyn). L-kyn bifurcates into two branches, where the one ends in kynurenic acid and the other undergoes a cascade of enzymatic reactions to result in NAD^+ synthesis.

kynurenine pathway is a major pathway in tryptophan catabolism and is responsible for the catabolism of 95% of all dietary tryptophan,[15] which is used in protein synthesis.[9] In tryptophan catabolism, L-tryptophan is degraded through a series of enzymatic reactions.[15–17] L-kynurenine (L-kyn) is central to the kynurenine pathway, which bifurcates and results in the formation of kynurenic acid (KA) or quinolinic acid (Quin),[14] where the latter can then be converted by to NAD^+ (Figure 1).[10]

Although melanoma is a rare type of cancer, accounting for less than 5% of all skin cancers,[18] it is among the deadliest as it accounts for 75% of skin cancer mortality.[19] Metabolites implicated in the kynurenine pathway, namely L-kyn and KA[14] previously displayed antiproliferative and cytotoxic effects in vitro against cancer cells.[20] Despite the growing interest in these compounds there are limited studies examining the in vitro effects of the exogenous treatment of melanoma with kynurenine metabolites. This study, therefore, aimed to investigate the effects of exogenous kynurenine compounds (L-kyn, Quin, and KA) on melanoma cells in vitro.

2 | MATERIALS AND METHODS

2.1 | Cell lines

This section will discuss the melanoma (B16 F10), the macrophage (RAW 264.7), and keratinocytes (HaCat) cell lines that were used in this study.

2.1.1 | Melanoma

The melanoma (B16 F10) cell line is isolated from the skin tissue of a mouse with melanoma and is characterized as a standard cell line for melanoma research.[21] The B16 F10 cell line was purchased from the American Type Culture Collection B16 F10 (ATCC® CRL-6475™) and used between passages 4 and 12.

2.1.2 | Monocyte/macrophage cells

The RAW 264.7 cell line was used as the control cell line. RAW 264.7 is a mouse, monocyte/macrophage-like cell line.[22] This cell line was purchased from CELLONEX, South Africa, and used between passages 6 and 20. In accordance with a previous study investigating the kynurenine pathway, the RAW 264.7 cell line was used as a control cell line,[23] since macrophages are known to express all the enzymes associated with the kynurenine pathway.[24]

2.1.3 | Keratinocyte cells

The HaCat cell line is a human keratinocyte cell line[25] and was used as a control cell line. This cell line was purchased from CELLONEX, South Africa, and used between passages 18 and 25.

2.2 | Sample preparation

Dimethyl sulfoxide (DMSO) at ≤0.1% volume per volume (v/v) was used as a solvent for kynurenine compounds (L-kyn, Quin, and KA) for crystal violet experiments. DMSO content of the final dilutions never exceeded 0.1% (v/v). L-kyn and KA were dissolved in <0.01% v/v DMSO and Quin in ≤0.1% v/v DMSO. Serial dilutions were made by adding 0.1 M phosphate-buffered saline (PBS) at (pH 7.4) to the treatments. The control samples for both cell lines, was exposed to the complete culture medium (CCM):PBS in a 1:1 ratio. A vehicle control of 0.1% (v/v) DMSO was also included for experiments with Quin-treated samples, as Quin was dissolved in the highest percentage DMSO (0.1% v/v). In addition, the current study focuses on the investigation of kynurenine metabolites on melanoma B16 F10 cells, with particular focus on these compounds' possible selective cytotoxic properties toward this melanoma cell line. Therefore, to effectively demonstrate the ability of kynurenine compounds to act as targeted therapies toward melanoma, all the results were compared to a nonselective cytotoxic agent, such as nocodazole. The positive control cells were, therefore, exposed to 1.30 mM nocodazole (NOC), which is a microtubule disruptor. NOC was dissolved in <0.01% v/v DMSO and diluted by adding ddH_2O to the treatments.

2.3 | General culture maintenance

The B16 F10, RAW 264.7, and HaCat cells were cultured in T25 or T75 cm^2 tissue culture flasks. All cell lines were cultured in CCM, consisting of Dulbecco's modified essential medium (DMEM) supplemented with 10% fetal calf serum (FCS) and 1% antibiotics (amphotericin/penicillin/streptomycin). These cells were cultured and maintained in sterile culture flasks at 37°C with 5% CO_2 in a Forma Scientific water-jacketed incubator, which provided a humidified atmosphere. Cells were allowed to grow until they reach 70% confluency, with a CCM change at 1- to 3-day intervals.

Upon reaching the desired confluency, the CCM was removed, and all cells were washed with 2 mL warm sterile 0.1 M PBS. The 0.1 M PBS was discarded, and 2 mL TrypLE™ Express phenol red was added to B16 F10 cells and 5% Trypsin was added to HaCat cells facilitate detachment of the cells. The cells exposed to TrypLE™ Express phenol red were incubated for 5 min and cells exposed to 5% Trypsin was incubated for 10 min. Detached B16 F10 and HaCat cells were neutralized with 4 mL CCM that was added to the flask. The RAW 264.7 cells were scraped with sterile cell scrapers and CCM was added to harvest the cells. The cell suspension of all cell lines was transferred to a 15 mL tube and centrifuged for 10 min at 3000 rpm after which the supernatant was discarded, and the cell pellet was resuspended in 1 mL of CCM. The resuspended cells were either seeded for experiments, cryopreserved in a 1:1 ratio in freeze medium (10% CCM, 10% DMSO in 80% fetal bovine serum) and stored at −80°C in cryovials or, reseeded into subcultures to be used in experiments. The passage of the cells was indicated on cryovials and newly seeded flasks. For all experimental purposes, cells were stained with a 0.1% trypan blue solution, and a hemocytometer was used to count viable cells. Laboratory sterile conditions were implemented.

2.4 | Crystal violet staining

Cells were seeded in 96-well plates at 5000 and 10,000 cells/well for B16 F10 (melanoma) and RAW 264.7 and HaCat (control) cells respectively. Cells were incubated for 24 h at 37°C and 5% CO_2 in a humidified incubator to allow cells to attach. After 24 h, the cells were exposed to serial dilutions of each compound (1–5 mM). The concentrations of kynurenine compounds were based on previously used concentrations in a range from 0 to 5 mM in vitro.[20]

Cells were exposed to kynurenine metabolites for 24, 48, and 72 h to observe cell viability over time in response to treatments. A vehicle control, DMSO at 0.1% (v/v) was included for experiments. After time-dependent exposure of each compound, the cells were fixed with 1% glutaraldehyde and further incubated for 30 min. The cells were then stained with 100 µL of 0.1% crystal violet at room temperature for 30 min. The plates were then rinsed in tap water, left to dry, and solubilized with 100 µL of 10% acetic acid and absorbance was measured at a wavelength of 570 nm and results were reported as the percentage cell viability in relation to the vehicle control (cells exposed to 0.1% DMSO) and the half maximal inhibitory concentration (IC_{50}) values were calculated using GraphPad Prism v6.01. The viability values of the concentration range of each compound were extrapolated and the IC_{50} values were calculated with the GraphPad Prism v6.01 software using nonlinear regression. The IC_{50} stated is the calculated IC_{50} derived from at least three wells from 3 biological repeats. For all subsequent experiments the calculated IC_{50} values obtained for B16 F10 cells at 48 h were used on B16 F10, RAW 264.7 and HaCat cells to determine the effects of compounds at IC_{50} values. In addition, the calculated IC_{50} values were further tested with the crystal violet assay in vitro to compare the calculated IC_{50} to its actual effect on all cell lines and make conclusions on selective cytotoxicity.

2.5 | Polarization-optical transmitted light differential interference contrast (PlasDIC) and hematoxylin and eosin (H&E) staining

Cells were seeded in 24-well plates, where B16 F10 cells were seeded at 10,000 cells/well and RAW 264.7 and HaCat cells were seeded at 20,000 cells/well. After allowing for attachment, all cell lines were exposed to various treatments (L-kyn, Quin, and KA) at IC_{50} values of B16 F10 cells and further incubated for 48 h. For PlasDIC, cells were

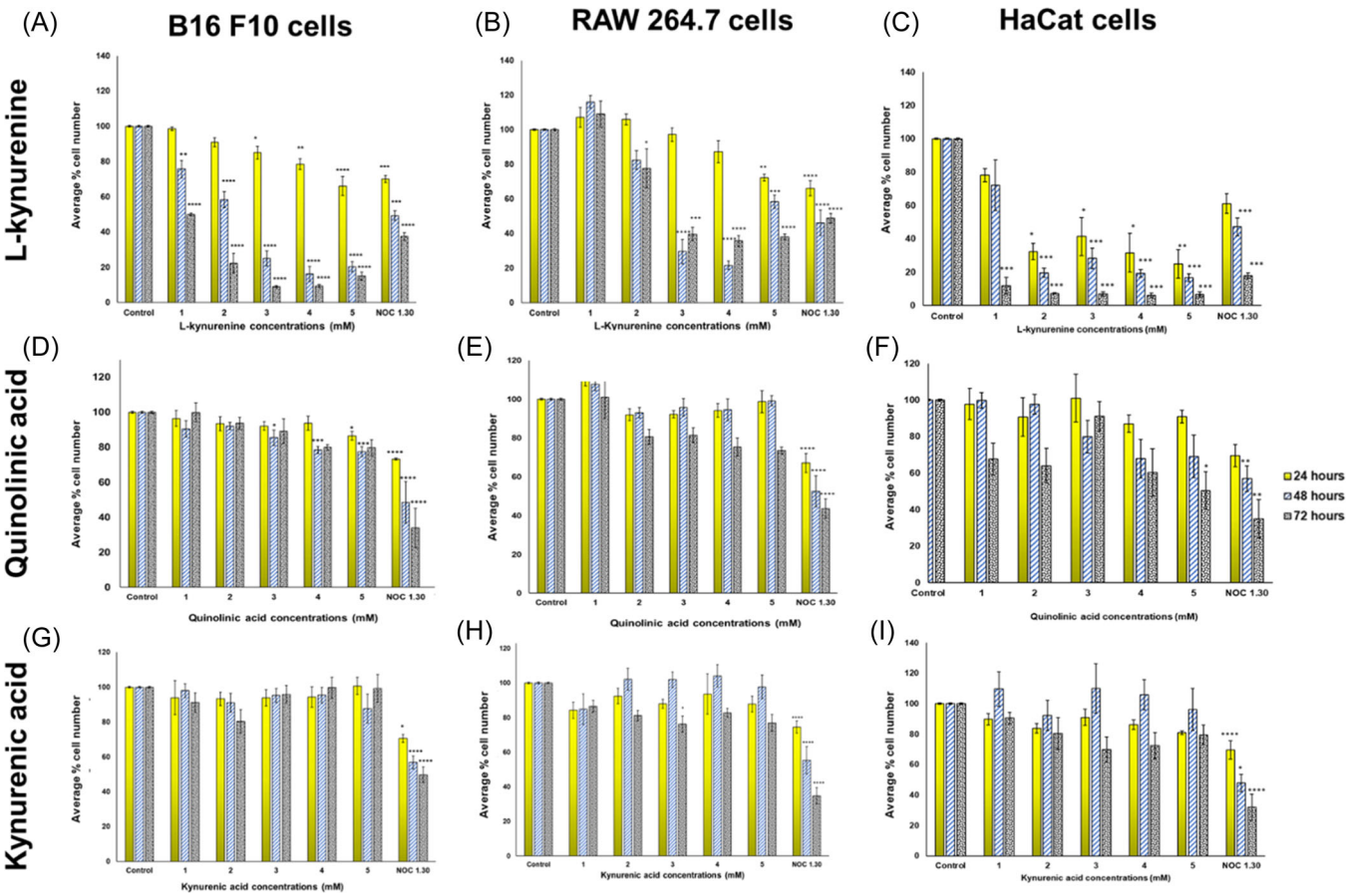

FIGURE 2 The effect of (A) L-kynurenine on the cell number of B16 F10, (B) RAW 264.7 and (C) HaCat, and the effect of quinolinic acid on the cell number of (D) B16 F10, (E) RAW 264.7 cells, and (F) Hacat cells and the effect of kynurenic acid on the cell number of (G) B16 F10, (H) RAW 264.7 cells, and (I) Hacat cells at 24, 48, and 72 h in vitro. Cell number values are expressed as the percentage relative to complete culture medium (CCM): ddH_2O or CCM: phosphate-buffered saline-treated control samples of at least three experimental repeats done in triplicate, with the standard error of mean indicated by the error bars. $^*p \le .05$; $^{**}p \le .01$; $^{***}p \le .001$; $^{****}p \le .0001$ indicates significant difference when compared to the control.

then viewed with a Zeiss inverted Axiovert CFL40 microscope (Zeiss) with a PlasDIC filter. After PlasDIC imaging, the medium was discarded, and the coverslips were covered with Bouin's fixative and left for 60 min at room temperature. The Bouin's fixative was discarded, and the coverslips were covered with 70% ethanol and left for 20 min at room temperature. This was followed by a rinse with tap water and thereafter the coverslips were covered in Mayer's hematoxylin and left for 20 min. A wash for 2 min in tap water followed then a rinse with 70% ethanol. The coverslips were then covered in eosin (1%) for 5 min then were dehydrated twice for 5 min with 70%, 96%, and 100% ethanol. Coverslips were then covered in xylene and left for 5 min and mounted on microscope slides with resin. After the coverslips were left to dry, the cells were viewed with the Zeis Axiovert MRc microscope (Zeis). and images were viewed at ×100 magnification with immersion oil. Images were captured with an imager Nikon Optiphot.

2.6 | Statistics

All experiments include at least three technical and three biological repeats. All quantitative data is represented as average ± standard error of mean (SEM). Data were checked for normality using the Shapiro–Wilks test and further tested for significant differences using one-way analysis of variance (ANOVA) with the Tukey test (if data were parametric) or the Kruskal–Wallis ANOVA with the Dunn test (if data was nonparametric). $p \leq .05$ was considered significant.

3 | RESULTS

3.1 | Cytotoxicity—IC_{50} determination

A vehicle control (0.1% v/v DMSO) was included for experiments with Quin-treated samples, as Quin contained the highest DMSO concentration of all compounds. No significant differences in cell proliferation were observed between CCM:ddH_2O or CCM:PBS and vehicle control (0.1% v/v DMSO) samples, implying a negligible effect of DMSO on cell proliferation. B16 F10 as well as RAW 264.7 cells, cells were exposed to L-kyn in a range from 0–5 mM. L-kyn displayed time-dependent cytotoxicity in B16 F10 cells, with statistically significant cytotoxic effects after 48 h at a concentration of 1 mM (Figure 2A). However, L-kyn only started to display significant cytotoxic effects in RAW 264.7 cells after 72 h at a concentration of 2 mM (Figure 2B). HaCats exposed to L-kyn presented with a similar trend of cytotoxicity as observed in B16 F10 cells (Figure 2C).

Quin displayed statistically significant cytotoxic effects in B16 F10 cells at 48 h from 3 to 5 mM (Figure 2C), but not in RAW 264.7 cells (Figure 2D). In HaCat cells, Quin-induced cytotoxicity after 72 h at 5 mM.

In B16 F10 as well as HaCat cells, KA did not display statistically significant cytotoxic effects (Figure 2G,I) but displayed cytotoxic effects in RAW 264.7 cells after 72 h at 3 mM (Figure 2H).

A summary of the calculated IC_{50} values for all compounds at 24, 48, and 72 h are shown in Table 1. When comparing the IC_{50} of B16

TABLE 1 Calculated IC_{50} values (mM) and IC_{50} ranges in B16 F10, RAW 264.7, and HaCat cells at 24, 48, and 72 h using data in a range from 0 to 5 mM.

Compound	Cell line								
	B16 F10			RAW 264.7			HaCat		
	24 h	48 h	72 h	24 h	48 h	72 h	24 h	48 h	72 h
L-kyn	13.64 (11.10–17.23)	1.74 (1.25–2.16)	0.68 (0.52–8.02)	31.06 (18.83–72.01)	3.54 (2.44–5.93)	2.22 (2.50–5.43)	1.810 (1.09– 2.90)	1.146 (0.790–1.61)	0.1627 (0.11–0.21)
Quin	37.09 (27.45–53.41)	8.23 (5.96–20.59)	20.44 (15.12–29.91)	89.36 (39.18–213.60)	68.08 (39.18–213.60)	11.61 (9.09–15.35)	43.31 (19.72–10798)	20.07 (12.25–42.71)	6.083 (3.85–10.28)
KA	89.80 (36.25–infinity)	21.52 (7.99–103.30)	76.40 (29.36–infinity)	29.94 (17.60–5.33)	5.242e+042 (-infinity to +infinity)	13.07 (10.19–17.47)	20.62 (15.87–28.37)	2.261e+036 (-infinity-+infinity)	11.04 (7.65–17.35)

Abbreviations: IC_{50}, half maximal inhibitory concentration; KA, kynurenic acid; L-kyn, L-kynurenine; Quin, quinolinic acid.

F10 cells to the RAW 264.7 control cells exposed to the B16 F10 IC_{50} at 48 h, less cell death was observed, approximately 2× less for L-kyn, 8× less for Quin and several fold times less for KA. When B16 F10 were compared to HaCat cells at 48 h, obtained IC_{50} values by L-kyn were similar, however for Quin it was 2× less, and for KA several fold times less. At 72 h IC_{50} values of the B16 F10 melanoma cells were similar to the RAW 264.7 and HaCat control cell lines. It was therefore decided that the 48 h timeline, was the ideal timeline to continue with.

The treatment of B16 F10, RAW 264.7, and HaCat cells with kynurenine metabolites at calculated IC_{50} values for B16 F10 cells for 48 h, demonstrated overall higher cell viability values for RAW 264.7 cells, except for KA. L-kyn at 1.74 mM induced an average cell viability value of 47.04% in B16 F10 cells,60.63% in RAW 264.7 cells, and 41.65% in HaCat cells. Quin at 8.23 mM induced and an average cell viability value of 59.98% in B16 F10 cells, 77.04% in RAW 264.7 cells, and 64.55% in HaCat cells. However, KA at 21.51 mM induced an average cell viability value of 30.45% in B16 F10 cells,23.07% in RAW 264.7 cells, and 94.96% in HaCat cells. NOC at 1.30 mM induced an average cell viability value of 53.27% in B16 F10 cells,15.72% in RAW 264.7 cells, and 59.61% in HaCat cells (Figure 3).

3.2 | PlasDIC

All cell lines displayed confluent and attached control cells (treated with PBS and ddH_2O), (Figure 4A,B,G,H,M,N). In B16 F10 cells, L-kyn at 1.74 mM induced cell protrusions, cell debris and apoptotic body formation (Figure 4C). KA at 21.52 mM induced compromised cell density, cell protrusions, cell debris, and apoptotic body formation (Figure 4D). Quin at 8.23 mM induced cell rounding, cell debris, and compromised cell density (Figure 4E). NOC at 1.30 mM induced compromised cell density, cell rounding, and apoptotic body formation (Figure 4F).

In RAW 264.7 cells, L-kyn at 1.74 mM induced cell rounding, compromised cell density, and apoptotic body formation (Figure 4I). KA at 21.52 mM induced compromised cell density, cell protrusions, and cell rounding (Figure 4J). Quin at 8.23 mM induced cell swelling, cell protrusions, and compromised cell density (Figure 4K). NOC at 1.30 mM induced signs of compromised cell density, cell rounding, cell protrusions, and apoptotic body formation (Figure 4L).

In HaCat cells, L-kyn at 1.74 mM induced cell rounding (Figure 4O). KA at 21.52 mM induced compromised cell density and membrane blebbing (Figure 4P). Quin at 8.23 mM did not influence cell morphology and cells remained confluent (Figure 4Q). NOC at

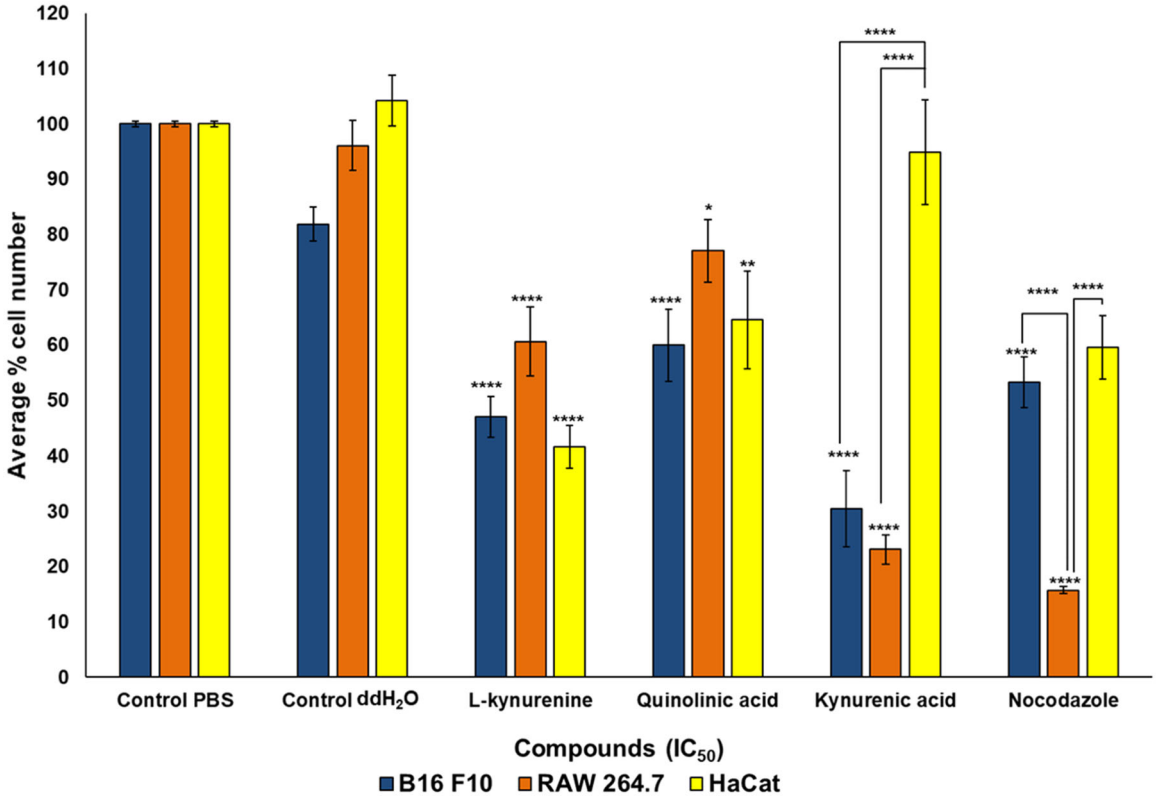

FIGURE 3 The effect of kynurenine compounds at half-maximal inhibitory concentration (IC_{50}) after 48 h on B16 F10, RAW 264.7, and HaCat cells in vitro. Cell number values are expressed as the percentage of cells relative to complete culture medium: phosphate-buffered saline-treated control samples of at least three experimental repeats done in triplicate, with the standard error of mean (SEM) indicated by the error bars. $^{**}p \leq .01$; $^{***}p \leq .001$; $^{****}p \leq .0001$ indicates significant difference when compared to the control.

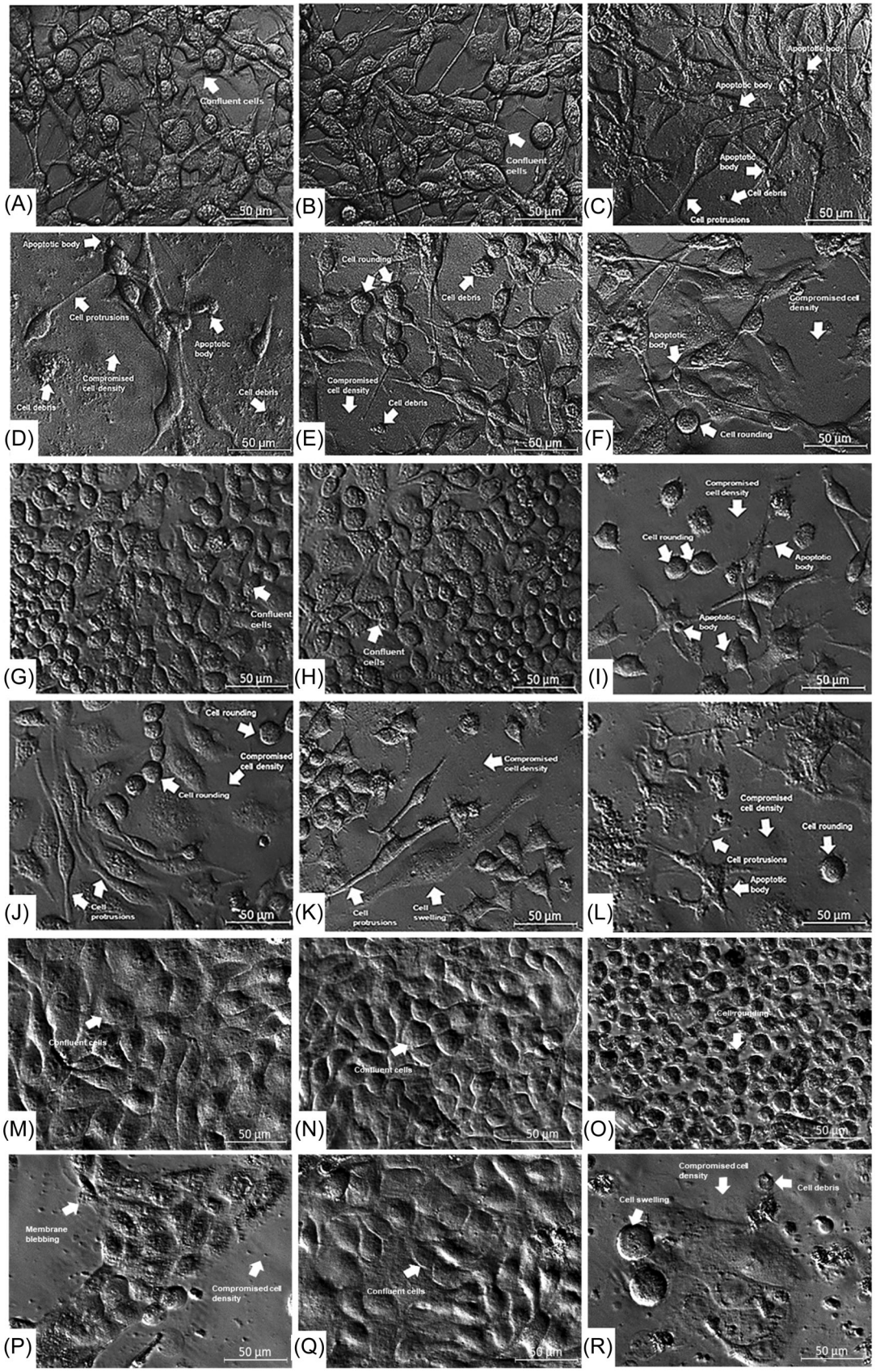

FIGURE 4 (See caption on next page).

1.30 mM induced signs of compromised cell density, cell debris, and cell swelling (Figure 4R).

3.3 | H&E staining

All cell lines displayed confluent and attached control cells (treated with PBS and ddH_2O), (Figure 5A,B,G,H,M,N). In B16 F10 cells, L-kyn at 1.74 mM induced membrane blebbing and apoptotic body formation (Figure 5C). KA at 21.52 mM induced signs of compromised cell density and cell rounding (Figure 5D). Quin at 8.23 mM induced cell swelling, cell protrusions, cell rounding, and apoptotic body formation (Figure 5E). NOC at 1.30 mM induced signs of cell swelling, compromised cell density, and apoptotic body formation (Figure 5F).

In RAW 264.7 cells, L-kyn at 1.74 mM induced cell rounding, compromised cell density, and karyorrhexis (nuclear fragmentation) (Figure 5I). KA at 21.52 mM induced compromised cell density, cell protrusions, and cell rounding (Figure 5J). Quin at 8.23 mM induced compromised cell density and karyorrhexis (Figure 5K). NOC at 1.30 mM induced compromised cell density, cell swelling, and apoptotic body formation (Figure 5L).

In HaCat cells, L-kyn at 1.74 mM induced cell rounding (Figure 5O). KA at 21.52 mM induced compromised cell density (Figure 5P). Quin at 8.23 mM did not influence cell morphology and cells remained confluent (Figure 5Q). NOC at 1.30 mM induced signs of cell swelling (Figure 5R).

4 | DISCUSSION

Exogenous exposure of kynurenine compounds to proliferating cells may elicit various effects, as metabolites implicated in the kynurenine pathway, namely L-kyn and KA previously displayed antiproliferative and cytotoxic effects in vitro against melanoma cells.[20] The cytotoxicity study using crystal violet staining by testing the physiological ranges of kynurenine metabolites on B16 F10, RAW 264.7, and HaCat cells, revealed that the calculated IC_{50} values for all metabolites are much higher than physiological concentrations, to induce cytotoxic effects toward B16 F10 melanoma cells. Marszalek-Grabska et al. previously reviewed physiological concentrations of L-kyn in body fluids and tissues, which ranges between 1.2 and 1.8 μM in human blood,[26] where KA was detected in the serum of patients diagnosed with cancer in a range from 21.3 to 250 nM depending on the type of cancer.[27] In this study, L-kyn, the central metabolite in the kynurenine pathway, was the most potent anticancer compound, compared to the two end metabolites, namely Quin and KA. These results can be explained by both the tryptophan depletion theory and the tryptophan utilization theory.

The tryptophan depletion theory first reiterates the essential role of tryptophan in cell proliferation and maintenance in physiological (e.g., immune cells) as well as pathological (e.g., cancer cells) conditions to fuel NAD^+ production.[6,28] However, NAD^+ production has both a positive and negative effect on cancer progression as it promotes both uncontrolled proliferation in cancer cells as well as an antitumour immune response by acting as a pro-inflammatory cytokine.[6] In the absence of adequate niacin intake, the catabolism of tryptophan acts as a secondary, salvage pathway for NAD^+ synthesis.[6] In this process, the depletion of tryptophan due to its catabolism, as a mechanism to increase NAD^+ production, has proved to promote tumor cell-intrinsic malignant properties as well as tumor immune escape.[29] Therefore, cancer patients with malignant tumors often present with depleted tryptophan levels, which correlates with disease progression and loss of immunocompetence.[30] As a result, the depletion of tryptophan during its catabolism, has been associated with T cell cycle arrest and the formation of metabolites, such as L-kyn, Quin, 3-hydroxykynurenine, and 3-hydroxyanthranilic acid, which previously suppressed T cell proliferation and induced apoptosis.[31] Despite describing its involvement in cancer progression, the tryptophan depletion theory of indoleamine 2,3 dioxygenase activation fails to explain the functions of the produced tryptophan metabolites during the process of catabolism. In addition, it was previously believed that kynurenine pathway metabolites have no function and are excreted in the urine.[9]

On the other hand, the tryptophan utilization theory suggests that cancer progression does not solely rely on tryptophan depletion, but also introduces the idea that metabolites produced during tryptophan catabolism, acts as active substances with specific receptor systems for each metabolite on different cell populations.[9,15] This theory supports the data from our study, which indicates that the exogenous administration of each kynurenine metabolite had a different effect on cytotoxicity in B16 F10, RAW 264.7, and HaCat cells. In addition, this current study found that L-kyn displayed the greatest cytotoxicity toward melanoma B16 F10

FIGURE 4 Polarization-optical transmitted light differential interference contrast micrographs of B16 F10 cells, RAW 264.7, and HaCat cells at 48 h after exposure to the B16 F10 half-maximal inhibitory concentration (IC_{50}) of various compounds. (A) control B16 F10 cells treated with phosphate-buffered saline (PBS), (B) control B16 F10 cells treated with ddH_2O, (C) L-kynurenine-treated B16 F10 cells at 1.74 mM, (D) kynurenic acid-treated B16 F10 cells at 21.52 mM, (E) quinolinic acid-treated B16 F10 cells at 8.23 mM (F) positive control B16 F10 cells treated with nocodazole (NOC) at 1.30 mM. (G) control RAW 264.7 cells treated with PBS, (H) control RAW 264.7 cells treated with ddH_2O, (I) L-kynurenine-treated RAW 264.7 cells at 1.74 mM, (J) kynurenic acid-treated RAW 264.7 cells at 21.52 mM, (K) quinolinic acid-treated RAW 264.7 cells at 8.23 mM (L) positive control RAW 264.7 cells treated with NOC at 1.30 mM, (M) control HaCat cells treated with PBS, (N) control HaCat cells treated with ddH_2O, (O) L-kynurenine-treated HaCat cells at 1.74 mM, (P) kynurenic acid-treated HaCat cells at 21.52 mM, (Q) quinolinic acid-treated HaCat cells at 8.23 mM (R) positive control HaCat cells treated with NOC at 1.30 mM. Micrographs were taken at ×40 magnification.

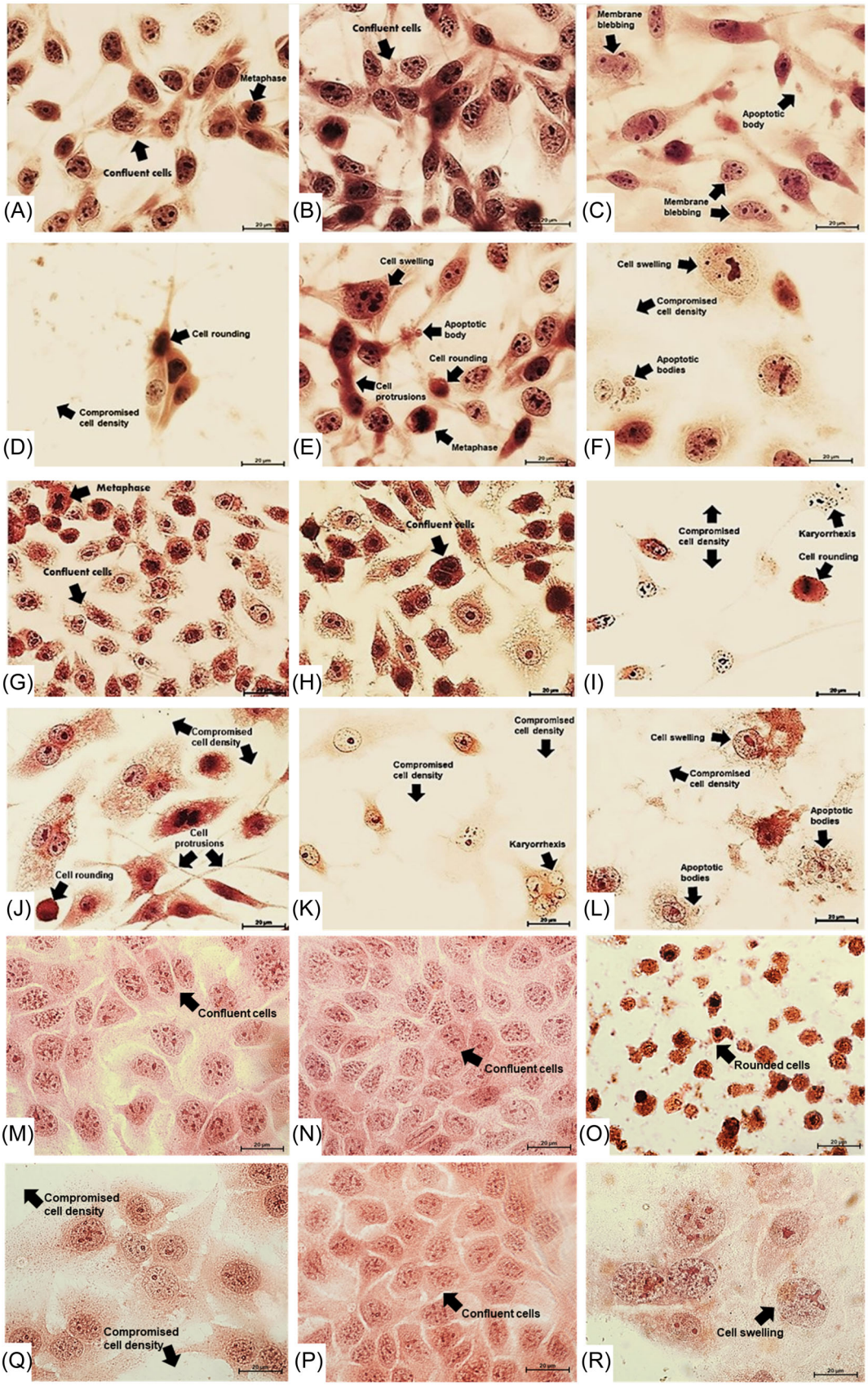

FIGURE 5 (See caption on next page).

cells and the normal HaCat keratinocyte cells in the millimolar (mM) range, whereas Quin and KA displayed less significant cytotoxic effects at these concentrations. This is further supported by a previous study where L-kyn (at 5 mM), but not KA exerted cytotoxicity against human melanoma A375 and RPMI7951 cells, measured by means of the Bromodeoxyuridine (BrdU) assay indicating the level of DNA synthesis.[20] The results from a study by Walczak et al., using the BrdU assay supported this statement by indicating that KA (at 5 mM) only moderately inhibited DNA synthesis (20.7%) in SK-MEL-3 cells (a cell line derived from melanoma metastasis), whereas L-kyn (at 5 mM) significantly inhibited DNA synthesis.[32]

L-kyn and KA are aryl hydrocarbon receptors (Ahr) ligands, and each may regulate the Ahr signaling pathway differently.[24] Hence, L-kyn may interfere with the downstream signaling pathway more effectively as compared to KA. A previous study suggested that Ahr agonists may display inconsistent behavior in different cells,[31] which explains our finding that KA did not display cytotoxicity against B16 F10 cells, even though it previously induced cytotoxic effects against other cancers, such as colon-derived cancer cells, human glioblastoma, and human renal cell carcinoma.[33–35] The authors, therefore, propose that Ahr activation may differ between B16 F10 and HaCat cell lines versus RAW 264.7 cell lines, thus giving rise to the differences in the effects observed.

In addition, the treatment with kynurenine compounds at 48-h IC_{50} values resulted in morphological changes in all three cell lines. Several features of apoptosis, such as cell rounding, cell shrinkage, chromatin condensation, nuclear fragmentation (karyorrhexis), and plasma membrane blebbing, were observed.[36–40] In addition, Quin-induced cell swelling in B16 F10 cells, which has previously been classified as a hallmark of necrosis,[40] but did not induce significant changes in the morphology of HaCat cells.

In conclusion, this study provides a better understanding of the in vitro cytotoxic effects of kynurenine exogenous compounds against B16 F10 melanoma cells and confirms that L-kyn, Quin, and KA each display different levels of cytotoxicity. Although this study included three cell lines, the study observed a limitation which was the similar cytotoxic effect induced by L-kyn on the cancerous B16 F10 and the noncancerous HaCat cells. Therefore, the authors suggest the inclusion of melanocytes as an additional control cell line for future studies. This study demonstrated that L-kyn was shown to be the most potent cytotoxic compound in all cell lines (B16 F10, RAW 264.7, and HaCat) and may offer future treatment strategies in combination with other viable treatments against melanoma. In vivo research on the kynurenine metabolites currently being conducted in our research group will assist to substantiate the findings of this study.

ACKNOWLEDGMENTS

The author(s) disclosed receipt of the following financial support for the research, authorship, and/or publication of this article: The Research Development program of Dr. Yvette Nkondo Hlophe and Dr. June Cheptoo Serem by the University of Pretoria. University of Pretoria, Physiology Head of Department, Prof. A. Joubert for funding to present this work at a national congress. School of Medicine Research Committee (RESCOM) Grant awarded to Ms Basson. National Research Foundation (NRF) awarded to Prof. R. Anguelov.

CONFLICT OF INTEREST STATEMENT

The authors declare no conflict of interest.

DATA AVAILABILITY STATEMENT

The data that support the findings of this study are available from the corresponding author upon reasonable request.

ORCID

Charlise Basson http://orcid.org/0000-0002-6123-9707
June Cheptoo Serem http://orcid.org/0000-0001-9912-166X
Yvette Nkondo Hlophe http://orcid.org/0000-0002-3112-2436
Priyesh Bipath http://orcid.org/0000-0002-5433-7069

REFERENCES

1. Chatterjee A, Rodger EJ, Eccles MR. Epigenetic drivers of tumourigenesis and cancer metastasis. *Sem Cancer Biol*. 2018;51:149-159.
2. Hassanpour SH, Dehghani M. Review of cancer from perspective of molecular. *J Cancer Res Pract*. 2017;4(4):127-129.
3. Vermeulen K, Van Bockstaele DR, Berneman ZN. The cell cycle: a review of regulation, deregulation and therapeutic targets in cancer. *Cell Prolif*. 2003;36(3):131-149.
4. Adjiri A. Tracing the path of cancer initiation: the aa protein-based model for cancer genesis. *BMC Cancer*. 2018;18(1):831.
5. Vincenzi B, Schiavon G, Silletta M, et al. Cell cycle alterations and lung cancer. *Histol. Histopathol*. 2006;21(4):423-435.
6. Navas LE, Carnero A. Nad^+ metabolism, stemness, the immune response, and cancer. *Signal Transduct Target Ther*. 2021;6(1):2.

FIGURE 5 Hematoxylin and eosin images of B16 F10 and RAW 264.7 cells at 48 h after exposure to the B16 F10 half-maximal inhibitory concentration of various compounds. (A) control B16 F10 cells treated with phosphate-buffered saline, (B) control B16 F10 cells treated with ddH_2O, (C) L-kynurenine-treated B16 F10 cells at 1.74 mM, (D) kynurenic acid-treated B16 F10 cells at 21.52 mM, (E) quinolinic acid-treated B16 F10 cells at 8.23 mM (F) positive control B16 F10 cells treated with nocodazole (NOC) at 1.30 mM. (G) control RAW 264.7 cells treated with PBS, (H) control RAW 264.7 cells treated with ddH_2O, (I) L-kynurenine-treated RAW 264.7 cells at 1.74 mM, (J) kynurenic acid-treated RAW 264.7 cells at 21.52 mM, (K) quinolinic acid-treated RAW 264.7 cells at 8.23 mM (L) positive control RAW 264.7 cells treated with NOC at 1.30 mM, (M) control HaCat cells treated with PBS, (N) control HaCat cells treated with ddH_2O, (O) L-kynurenine-treated HaCat cells at 1.74 mM, (P) kynurenic acid-treated HaCat cells at 21.52 mM, (Q) quinolinic acid-treated HaCat cells at 8.23 mM (R) positive control HaCat cells treated with NOC at 1.30 mM. Micrographs were taken at ×100 magnification.

7. Zhang W, Zhang S-L, Hu X, Tam KY. Targeting tumor metabolism for cancer treatment: is pyruvate dehydrogenase kinases (PDKs) a viable anticancer target? *Int J Biol Sci*. 2015;11(12):1390-1400.
8. Liberti MV, Locasale JW. The warburg effect: how does it benefit cancer cells? *Trends Biochem Sci*. 2016;41(3):211-218.
9. Moffett JR, Namboodiri MA. Tryptophan and the immune response. *Immunol Cell Biol*. 2003;81(4):247-265.
10. Kulikova VA, Gromyko DV, Nikiforov AA. The regulatory role of NAD in human and animal cells. *Biochemistry (Mosc)*. 2018;83(7):800-812.
11. Kirkland JB. Niacin and carcinogenesis. *Nutr Cancer*. 2003;46(2):110-118.
12. Mehmel M, Jovanović N, Spitz U. Nicotinamide riboside-the current state of research and therapeutic uses. *Nutrients*. 2020;12(6):1616.
13. Moffett JR, Arun P, Puthillathu N, et al. Quinolinate as a marker for kynurenine metabolite formation and the unresolved question of NAD+ synthesis during inflammation and infection. *Front Immunol*. 2020;11:31.
14. Macchiarulo A, Camaioni E, Nuti R, Pellicciari R. Highlights at the gate of tryptophan catabolism: a review on the mechanisms of activation and regulation of indoleamine 2,3-dioxygenase (IDO), a novel target in cancer disease. *Amino Acids*. 2008;37:219-229.
15. Austin CJD, Rendina LM. Targeting key dioxygenases in tryptophan–kynurenine metabolism for immunomodulation and cancer chemotherapy. *Drug Discov Today*. 2015;20(5):609-617.
16. Zhai L, Ladomersky E, Lenzen A, et al. Ido1 in cancer: a Gemini of immune checkpoints. *Cell Mol Immunol*. 2018;15(5):447-457.
17. Campbell BM, Charych E, Lee AW, Möller T. Kynurenines in CNS disease: regulation by inflammatory cytokines. *Front Neurosci*. 2014;8:12.
18. Rebecca VW, Somasundaram R, Herlyn M. Pre-clinical modeling of cutaneous melanoma. *Nat Commun*. 2020;11(1):2858.
19. Davis LE, Shalin SC, Tackett AJ. Current state of melanoma diagnosis and treatment. *Cancer Biol Ther*. 2019;20(11):1366-1379.
20. Walczak K, Langner E, Makuch-Kocka A, et al. Effect of tryptophan-derived AHR ligands, kynurenine, KA and FICZ, on proliferation, cell cycle regulation and cell death of melanoma cells-in vitro studies. *Int J Mol Sci*. 2020;21(21):7946.
21. Couto GK, Segatto NV, Oliveira TL, Seixas FK, Schachtschneider KM, Collares T. The melding of drug screening platforms for melanoma. *Front Oncol*. 2019;9(9):512.
22. Kong L, Smith W, Hao D. Overview of raw264.7 for osteoclastogensis study: phenotype and stimuli. *J Cell Mol Med*. 2019;23(5):3077-3087.
23. Sundaram G, Brew BJ, Jones SP, et al. Quin toxicity on oligodendroglial cells: relevance for multiple sclerosis and therapeutic strategies. *J Neuroinflammation*. 2014;13(11):204.
24. Guillemin GJ, Smith DG, Smythe GA, et al. Expression of the kynurenine pathway enzymes in human microglia and macrophages. *Adv Exp Med Biol*. 2003;527:105-112.
25. Wilson VG. Growth and differentiation of HaCaT keratinocytes. *Methods Mol Biol*. 2014;1195:33-41.
26. Marszalek-Grabska M, Walczak K, Gawel K, et al. Kynurenine emerges from the shadows—current knowledge on its fate and function. *Pharmacol Ther*. 2021;225:107845.
27. Walczak K, Wnorowski A, Turski WA, Plech T. Kynurenic acid and cancer: facts and controversies. *Cell Mol Life Sci*. 2020;77(8):1531-1550.
28. Peyraud F, Guegan J-P, Bodet D, Cousin S, Bessede A, Italiano A. Targeting tryptophan catabolism in cancer immunotherapy era: challenges and perspectives. *Front Immunol*. 2022;13:807271.
29. Opitz CA, Somarribas Patterson LF, Mohapatra SR, et al. The therapeutic potential of targeting tryptophan catabolism in cancer. *Br J Cancer*. 2020;122(1):30-44.
30. Sucher R, Kurz K, Weiss G, Margreiter R, Fuchs D, Brandacher G. IDO-mediated tryptophan degradation in the pathogenesis of malignant tumor disease. *Int J Tryptophan Res*. 2010;3:113-120.
31. Nkandeu DS, Basson C, Joubert AM, et al. The involvement of a chemokine receptor antagonist CTCE-9908 and kynurenine metabolites in cancer development. *Cell Biochem Funct*. 2022;40(6):608-622.
32. Walczak K, Kazimierczak P, Szalast K, Plech T. UVB radiation and selected tryptophan-derived AhR ligands—potential biological interactions in melanoma cells. *Int J Mol Sci*. 2021;22(14):7500.
33. Walczak K, Dąbrowski W, Langner E, et al. Kynurenic acid synthesis and kynurenine aminotransferases expression in colon derived normal and cancer cells. *Scand J Gastroenterol*. 2011;46(7-8):903-912.
34. Walczak K, Deneka-Hannemann S, Jarosz B, et al. Kynurenic acid inhibits proliferation and migration of human glioblastoma T98G cells. *Pharmacol Rep*. 2014;66(1):130-136.
35. Walczak K, Żurawska M, Kiś J, et al. Kynurenic acid in human renal cell carcinoma: its antiproliferative and antimigrative action on Caki-2 cells. *Amino Acids*. 2012;43(4):1663-1670.
36. Elmore S. Apoptosis: a review of programmed cell death. *Toxicol Pathol*. 2007;35(4):495-516.
37. Chen Y, Hua Y, Li X, Arslan IM, Zhang W, Meng G. Distinct types of cell death and the implication in diabetic cardiomyopathy. *Front Pharmacol*. 2020;11:42.
38. Shi Y. Mechanisms of caspase activation and inhibition during apoptosis. *Mol Cell*. 2002;9(3):459-470.
39. Taylor RC, Cullen SP, Martin SJ. Apoptosis: controlled demolition at the cellular level. *Nat Rev Mol Cell Biol*. 2008;9(3):231-241.
40. Kim R, Emi M, Tanabe K. The role of apoptosis in cancer cell survival and therapeutic outcome. *Cancer Biol Ther*. 2006;5(11):1429-1442.

How to cite this article: Basson C, Serem JC, Hlophe YN, Bipath P. An in vitro investigation of L-kynurenine, quinolinic acid, and kynurenic acid on B16 F10 melanoma cell cytotoxicity and morphology. *Cell Biochem Funct*. 2023;41:912-922. doi:10.1002/cbf.3843